frontiers | Frontiers in Environmental Science

ORIGINAL RESEARCH
published: 30 June 2022
doi: 10.3389/fenvs.2022.912385

Quiet New Particle Formation in the Atmosphere

Markku Kulmala[1,2,3], Heikki Junninen[4], Lubna Dada[1,5], Imre Salma[6], Tamás Weidinger[7], Wanda Thén[8], Máté Vörösmarty[8], Kaupo Komsaare[4], Dominik Stolzenburg[1], Runlong Cai[1], Chao Yan[1,2,3], Xinyang Li[1], Chenjuan Deng[9], Jingkun Jiang[9], Tuukka Petäjä[1,3], Tuomo Nieminen[1,10] and Veli-Matti Kerminen[1]*

[1]Faculty of Science, Institute for Atmospheric and Earth System Research (INAR) / Physics, University of Helsinki, Helsinki, Finland, [2]Aerosol and Haze Laboratory, Beijing Advanced Innovation Center for Soft Matter Sciences and Engineering, Beijing University of Chemical Technology (BUCT), Beijing, China, [3]Joint International Research Laboratory of Atmospheric and Earth System Sciences, School of Atmospheric Sciences, Nanjing University, Nanjing, China, [4]Institute of Physics, University of Tartu, Tartu, Estonia, [5]Laboratory of Atmospheric Chemistry, Paul Scherrer Institute, Villigen, Switzerland, [6]Institute of Chemistry, Eötvös Loránd University, Budapest, Hungary, [7]Department of Meteorology, Eötvös Loránd University, Budapest, Hungary, [8]Hevesy György Ph. D. School of Chemistry, Eötvös Loránd University, Budapest, Hungary, [9]State Key Joint Laboratory of Environment Simulation and Pollution Control, State Environmental Protection Key Laboratory of Sources and Control of Air Pollution Complex, School of Environment, Tsinghua University, Beijing, China, [10]Faculty of Agriculture and Forestry, Institute for Atmospheric and Earth System Research (INAR)/Forest Sciences, University of Helsinki, Helsinki, Finland

OPEN ACCESS

Edited by:
Shanhu Lee,
University of Alabama in Huntsville, United States

Reviewed by:
Li-Hao Young,
China Medical University, Taiwan
Suzanne Crumeyrolle,
UMR8518 Laboratoire d'optique Atmosphèrique (LOA), France

***Correspondence:**
Markku Kulmala
markku.kulmala@helsinki.fi

Specialty section:
This article was submitted to Atmosphere and Climate, a section of the journal Frontiers in Environmental Science

Received: *05 April 2022*
Accepted: *01 June 2022*
Published: *30 June 2022*

Citation:
Kulmala M, Junninen H, Dada L, Salma I, Weidinger T, Thén W, Vörösmarty M, Komsaare K, Stolzenburg D, Cai R, Yan C, Li X, Deng C, Jiang J, Petäjä T, Nieminen T and Kerminen V-M (2022) Quiet New Particle Formation in the Atmosphere. Front. Environ. Sci. 10:912385. doi: 10.3389/fenvs.2022.912385

Atmospheric new particle formation (NPF) has been observed to take place in practice all around the world. In continental locations, typically about 10–40% of the days are so-called NPF event days characterized by a clear particle formation and growth that continue for several hours, occurring mostly during daytime. The other days are either non-event days, or days for which it is difficult to decide whether NPF had occurred or not. Using measurement data from several locations (Hyytiälä, Järvselja, and near-city background and city center of Budapest), we were able to show that NPF tends to occur also on the days traditionally characterized as non-event days. One explanation is the instrument sensitivity towards low number concentrations in the sub-10 nm range, which usually limits our capability to detect such NPF events. We found that during such days, particle formation rates at 6 nm were about 2–20% of those observed during the traditional NPF event days. Growth rates of the newly formed particles were very similar between the traditional NPF event and non-event days. This previously overlooked phenomenon, termed as quiet NPF, contributes significantly to the production of secondary particles in the atmosphere.

Keywords: classification of NPF events, long-term observations, instrument sensitivity, aerosol production, clustering, NPF events

INTRODUCTION

Changing climate and problems in air quality are globally crucial for both the humankind and the environment (e.g. Fiore et al., 2012; Boucher et al., 2013; Apte et al., 2015; IPCC, 2021). Understanding the complex interlinks between air quality and climate requires detailed information on atmospheric aerosol particles, including their concentrations, size distribution and chemical composition, as well as non-linear processes in their dynamics (e.g. Pöschl, 2005; Arneth et al., 2009; Samset, 2018; Rose et al., 2021). In the global atmosphere, the majority of the aerosol particle number load is due to atmospheric new particle formation (Spracklen et al., 2006; Yu

and Luo, 2009; Gordon et al., 2017) and the population-weighted fine particle matter ($PM_{2.5}$) load is largely, if not dominantly, due to gas-to-particle conversion (GTP) taking place in the atmosphere (Philip et al., 2014; Weagle et al., 2018). By producing new aerosol particles and secondary particulate matter, atmospheric NPF and GTP modify the number concentration, size distribution, chemical composition, and mass loading of atmospheric aerosol particle populations, thereby having close associations with both air quality and climate. NPF and GTP are, therefore, key phenomena for our understanding of aerosol source processes, interactions, transformation, effects and feedbacks in the atmosphere.

Atmospheric NPF has been observed to take place practically all over the world (Kulmala et al., 2004a; Kulmala and Kerminen, 2008; Wang et al., 2017; Kerminen et al., 2018; Nieminen et al., 2018; Chu et al., 2019; Bousiotis et al., 2021). The prevailing view is that this phenomenon is dominated by regional-scale NPF events that tend to occur during daytime and last for a few hours (Hussein et al., 2009; Dai et al., 2017; Kerminen et al., 2018; Németh et al., 2018; Kalkavouras et al., 2021). During such events, newly formed aerosol particles appear at diameters smaller than a few nm, after which these particles grow in size, often reaching the Aitken mode (25–100 nm) during the same day. The days characterized by NPF events, called NPF event days, have frequencies ranging from a few % up to 90% in the continental atmosphere, with typical NPF frequencies being between 10 and 40% (Kerminen et al., 2018; Nieminen et al., 2018; Chu et al., 2019; Bousiotis et al., 2021). However, there are also days showing a presence of sub-10 nm particles without any apparent particle growth (e.g. Buenrostro Mazon et al., 2009; Dada et al., 2018), originally termed as undefined days (Dal Maso et al., 2005). Lastly, a large fraction of days does not show any indications of particle formation or growth, and such days have traditionally been called as non-event days (e.g. Dal Maso et al., 2005; Kulmala et al., 2012; Dada et al., 2018).

New particle formation is initiated by molecular clustering, and this phenomenon appears to take place practically everywhere and all the time in the atmosphere (Kulmala et al., 2013; Kontkanen et al., 2017; Deng et al., 2021; Kulmala et al., 2022a). Several reasons have been identified why the continuous atmospheric clustering will lead to the substantially less frequent occurrence of NPF events. First, there are strong indications that the vapors governing cluster formation do not usually produce growing nanoparticles, but rather that a second group of vapors is needed to heterogeneously nucleate on small clusters or start to contribute to the growth *via* nano-Köhler type processes (Kulmala et al., 2004b; Tröstl et al., 2016). Second, molecular clusters growing in size need to survive their coagulation scavenging by larger, pre-existing aerosol particles to be able to form a particle population characteristic of observed NPF events (McMurry and Friedlander, 1979; Kerminen et al., 2001; Pierce and Adams, 2007). Kulmala et al. (2017) investigated theoretically the survival of growing molecular clusters and nanoparticles in different environments, and concluded that, contrary to observations, NPF events should not be possible in highly polluted conditions. The only explanation for this discrepancy is our incomplete understanding of the dynamics of sub-5 nm clusters/particles, including their real growth rate and the efficiency by which they are scavenged by larger particles (Kulmala et al., 2017; Tuovinen et al., 2020).

The findings that NPF events can take place under conditions usually thought to be highly unfavorable for the survival of the growing molecular clusters raises two important questions not investigated previously: 1) is it more generally applicable that atmospheric NPF occurs more frequently than believed, including the days traditionally characterized as non-event days? and 2) in case NPF does occur on such days, how much this "quiet NPF" will contribute to particle numbers present in the atmosphere? In this paper, we aim to provide plausible answers to these questions by investigating how intensively nanoparticles are being produced during days characterized as non-event days using current classification criteria. Our analysis is based on long-term measurements made at four continental sites. We start by discussing the detection of particle formation on days with no visible NPF using the current instruments and methods, after which we compare particle formation and growth rates associated with the "quiet NPF" to those observed on traditional NPF event days. We focus on particles larger than 6 nm in diameter in this comparison, partly because of the scarcity of measurement data from smaller sizes, and partly because of the above-mentioned deficiencies in our understanding of the dynamics of smaller particles.

METHODS

Measurement Sites and Instrumentation

In our analyses, we evaluate the data from two rural sites (the SMEAR II station in Hyytiälä, Finland, Hari and Kulmala, 2005), and the SMEAR Estonia station in Järvselja, Estonia, Noe et al., 2015), and from both near-city background site and city center in Budapest, Hungary (Salma et al., 2016a; Salma et al., 2016b). These four sites were selected because they have continuous measurement data covering a minimum of one year. At all the sites, identification and classification of regional NPF events and non-events were performed using daily particle number size distribution surface plots, as suggested by Dal Maso et al. (2005) and refined by Kulmala et al. (2012).

The SMEAR II station (Station for Measuring Ecosystem–Atmosphere Relations) is located in Hyytiälä (61.1° N, 24.17° E; 181 m above mean see level, a.s.l.; Hari and Kulmala, 2005), southern Finland. The site represents a semi-pristine boreal forest environment. Here we used two measurement data sets, the first one covering the years 2010–2020, and the second one covering the years 1997–2007. For the later period, we compared the very clear and uninterrupted (classified as type Ia events according to Dal Maso et al., 2005) NPF event days (N = 21) with non-event days (N = 1361). In analyzing the earlier period, we used all the classified events, including 973 NPF event days and 1184 non-event days. The particle number size

distribution data used in this study from the Hyytiälä site were measured from 3 to 1000 nm by a laboratory-built differential mobility particle sizer (DMPS, Aalto et al., 2001).

The SMEAR-Estonia measurement station (58°16′ N, 27°16′ E, 36 m a.s.l.; Noe et al., 2011, 2015) is located near Järvselja, a village with fewer than 50 inhabitants, in Estonia. The site is situated in the hemi-boreal forest zone with a moderately cool and moist climate by continental air masses from Siberian plains and Northern Fennoscandia, or by maritime influence from the Baltic Sea and the Lake Peipus. The site is surrounded by a mixed forest and wetland. The particle number size distributions (in a diameter range from 0.8 to 42 nm according to Millikan formula) were measured using a Neutral cluster and Air Ion Spectrometer (NAIS; Mirme et al., 2007; Manninen et al., 2009; Mirme and Mirme, 2013) and Electrical Aerosol Spectrometer (in a diameter range from 3 to 10000 nm, EAS; Tammet et al., 2002) during 2016–2020. NAIS and EAS both uses positive corona charger for charging particles for detection and negative precharger to neutralize them before charging. NAIS also allows to measure naturally charged particles, called air ions, when chargers are switched off. We investigated NAIS air ion size distribution data to calculate growth rates (GRs) for newly formed particles (**Supplementary Figure S9**), since it enables to see the evolution of newly formed particles also below 3 nm and the fact that air ions contribute to NPF, especially in the early stages (Iida et al., 2006; Kerminen et al., 2007). A total of 38 type Ia NPF event days and 749 non-event days were used in the analysis.

Budapest has 2.3 million inhabitants in the metropolitan area and has a central geographical location in the plain part of the Carpathian Basin. The measurements were performed at two distinct urban sites. The near-city background site is located at the north-western border of Budapest in a wooded area of the Konkoly Astronomical Observatory (47° 30′ 00″ N, 18° 57′ 47″ E., 478 m a.s.l., Salma et al., 2016b) of the Hungarian Academy of Sciences. The site is characterized by air masses that enter the city, as the prevailing wind direction in the area is north-westerly. The measurement data covers one full year from 19 January 2012 to 18 January 2013. The total number of type Ia NPF events was 43 and there were 231 non-event days involved in the analysis. Measurements in the city center site were accomplished at the Budapest platform for Aerosol Research and Training (BpART) Laboratory (N 47° 28′ 30″ N, 19° 3′ 45″ E, 115 m a.s.l., Salma et al., 2016a) of the Eötvös Loránd University. The site represents a well-mixed average atmospheric environment for the overall city center. The measurement data cover over 7 years: from 3 November 2008 to 2 November 2009, from 13 November 2013 to 12 November 2016, and from 28 January 2017 to 27 January 2020. The data with similar diameter bins were included in the analysis, and they involved 290 NPF event days and 1412 non-event days. The measurements in Budapest were realized by a flow-switching-type DMPS in a diameter range from 6 to 1000 nm in 27 size channels in the dry state (RH<30%) of particles with a time resolution of 8 min. Further details of the measuring system were described earlier (e.g. Salma and Németh, 2019). The measurements were conducted according to the international technical standard (Wiedensohler et al., 2012).

Detection of the Quiet Particle Formation and Subsequent Particle Growth

Atmospheric NPF events are described as sudden bursts of nucleation mode particles, typically around 3–5 nm in diameter, and their subsequent growth to the Aitken mode. Usually, the burst of new particles increases the concentration of nucleation mode particles from 1–10 cm^{-3} to a range of 10^2–10^5 cm^{-3} within a few hours. These events are easily detected by aerosol sizing instruments such as the DMPS and NAIS (Aalto et al., 2001; Mirme et al., 2007; Manninen et al., 2009). The detection of the growth nanometer-size particles by gravimetric methods is not suitable as the collectable mass increment during the few-hour period in these particles in the atmosphere is negligible. Instead, the particles can be detected and measured by methods based on electric principles. Electrical detection, however, includes considerable losses due to sampling and low charging efficiency of particles. The detection limit of nanoparticles, in terms of $dN/d\log D_p$ (where N is the count of particles in a size channel and D_p is the particle diameter) ranges between 10 and 1000 cm^{-3} around 2 nm depending on the used instrumentation (Kangasluoma et al., 2020). One way to increase the signal-to-noise ratio and thereby the detection efficiency, is to increase the sampling time (Stolzenburg et al., 2017; Cai et al., 2019).

The longest continuous time series of particle number size distribution measurements is available from the SMEAR II station in Hyytiälä. Since January 1996, about 15–30% and 25–50% of all days were NPF event days and non-event days, respectively on an annual scale (Nieminen et al., 2014; Nieminen et al., 2018), whereas the remaining fraction of the days could not be clearly classified to either of these two categories. NPF events can also be common in large cities and even megacities (Kulmala et al., 2017; Kerminen et al., 2018; Chu et al., 2019; Kulmala et al., 2021; Salma et al., 2021; Kulmala et al., 2022b). For example, the mean annual frequency of NPF events in Budapest was (21 ± 4)% for 10 years (Salma et al., 2021). In addition, it was shown that for this city and its region, the Carpathian Basin, the observed NPF events usually take place over a larger territory (Németh and Salma, 2014), forming a spatially coherent regional atmospheric phenomenon (Salma et al., 2016b). Local, small-scale NPF events are sometimes superimposed onto a regional NPF event in Budapest, which results in growth curves with multiple or broad onsets. The dynamic and timing properties of the two types of the NPF events show, however, considerable differences (Salma et al., 2016b; Salma and Németh, 2019). In such complex cases, the regional (large-scale) NPF events were retained in the analyses conducted here, since the occurrence frequency of the local NPF events was much smaller (ca. 4% of all events), and since their dynamic properties represent only constrained spatial and time scales (Salma et al., 2016a).

Since the formation of atmospheric aerosol particles is strongly dependent on solar radiation (Dada et al., 2017; Kerminen et al., 2018), the strength of this phenomenon tends to have a strong diurnal behavior. However, the sensitivity

towards small number concentrations with an individual instrument on a single day is often limited due to high diffusional losses, low detection efficiencies and temporally and spatially variable number concentrations, especially in the crucial sub-10 nm size-range. One way to increase the sampling time and to improve the signal-to-noise ratio is to average the signal over multiple days. We did this procedure separately for NPF event days and non-event days, and thereby obtained an average time evolution of the particle number size distribution for both types of the days.

An "average" NPF event day from the SMEAR II station in Hyytiälä is shown in **Supplementary Figure S1**. The time evolution of the particle number size distribution during such a day displays a similar growth pattern for newly formed particles as is common for individual NPF event days. The "average" non-event day (**Supplementary Figure S2**) shows no sign of particle growth, as expected. However, the situation changes after normalizing the data. When looking separately at each aerosol size bin, we may notice clearly enhanced concentrations during the daytime. We then normalize each size bin into the range of 0–1, so that only the shape of the particle number size distribution at any time of the day matters. By combining these scaled size bins into a surface plot, we can notice that the maxima of larger-diameter size bins appear later during the day compared with smaller-diameter size bins. For an "average" NPF event day scaled in this way, we can directly identify a particle formation and growth behavior similar to those on individual NPF event days (**Supplementary Figure S3**). For an "average" non-event day scaled this way, we can identify a growth pattern that is similar to that on individual NPF event days (**Supplementary Figure S4**).

Supplementary Figures S3, S4 make it possible to determine "average" particle growth rates on both NPF event and non-event days. However, we can also look at the temporal behavior of particle number concentration maxima in individual size bins (**Supplementary Figure S5**), and by that way define the growth rate (**Supplementary Figure S6**). By normalization, we get rid of the fact that on non-event days the signal is very low in the smallest size channels, often below the detection limit on a single day. Only the normalization enables us to detect the banana plot and to identify the particle growth. However, it is important to note that when we use the maximum concentration or appearance time (Hirsikko et al., 2005; Lehtipalo et al., 2014; Dada et al., 2020) for growth analysis we also investigate the signal of an individual size class and its time evolution. Therefore, the growth rate shown in **Supplementary Figure S6** is obtained exactly in the same manner as using the maximum concentration method (or appearance time method) applied to normal NPF event days.

The formation rates of 6-nm particles were calculated using the balance equation proposed by Kulmala et al. (2012) for particles in the size range of 6–25 nm:

$$J_6 = \frac{dN_{6-25}}{dt} + \mathrm{CoagS} \times N_{6-25} + \frac{\mathrm{GR}}{\Delta d_p} \times N_{6-25}. \quad (1)$$

Here, CoagS is the coagulation sink term calculated from the size-dependent pre-existing particle population, GR is the particle growth rate in the diameter range of 6–25 nm, and Δd_p is the difference in diameters between the upper and lower end of the size bin, here 6 and 25 nm, respectively. For consistency, the quantities in **Eq. 1** are acquired from the averaged NPF event and non-event days for the locations.

RESULTS AND DISCUSSION

The previously overlooked phenomenon investigated here, termed "quiet NPF", is taking place outside periods of traditional, regional NPF events. This can be seen either by analyzing long measurement time series where several years of data can be averaged, or by focusing on situations where the boundary layer is extremely stable, like at wetland sites at night (Junninen et al., 2022). Such quiet NPF is not easy to detect but, due to its apparently frequent occurrence, it might produce significant number concentrations of new aerosol particles in comparison with the traditional, regional NPF events.

General Behavior of Quiet NPF

We started our analysis using measurement data from the SMEAR II station in Hyytiälä (**Figure 1**). The results show that, after normalizing particle number size distributions and averaging them over a large number of days (*Detection of the Quiet Particle Formation and Subsequent Particle Growth Section*), we were able to identify a relatively similar "banana" type particle growth behavior for both NPF event and non-event days (**Figures 1A,C**). Interestingly, the average growth rate of 6–25 nm particles was only slightly lower on non-event days compared with NPF event days (**Table 1**). Particle formation rates at 3 and 6 nm, J_3 and J_6, showed larger differences between the NPF event and non-event days (**Figures 1B,D**). First, while the daytime particle formation rates have a relatively clear maximum at around noon on NPF event days, they seem to be flatter with a later afternoon maximum on non-event days. Second, as expected, the absolute values of particle formation rates are clearly lower for non-event days, especially during daytime. In order to test our algorithm further, we utilize an additional data set, including the data from 1997–2007, and event types Ia, Ib and II. Here, we first interpolate all the measured particle number size-distributions to 20 size bins logarithmically equally in diameter space, and then average the data to 1-h time resolution using median filtering. These datasets are averaged separately for NPF event and non-event days, and the daily averaged size-distributions are finally normalized (**Supplementary Figures S3, S4**). We find that the results from either method are quite similar in terms of GR and J (**Table 1**).

The diurnal evolution of normalized particle number size distributions during the "average" NPF event and non-event days in Budapest and Järvselja (**Supplementary Figures S7–S9**) were qualitatively similar to those in Hyytiälä, all displaying the "banana"-type growth behavior. In both Budapest and Järvselja, the average particle growth rates in non-event days were comparable to or slightly lower than those on NPF event days (**Table 1**), and the average particle

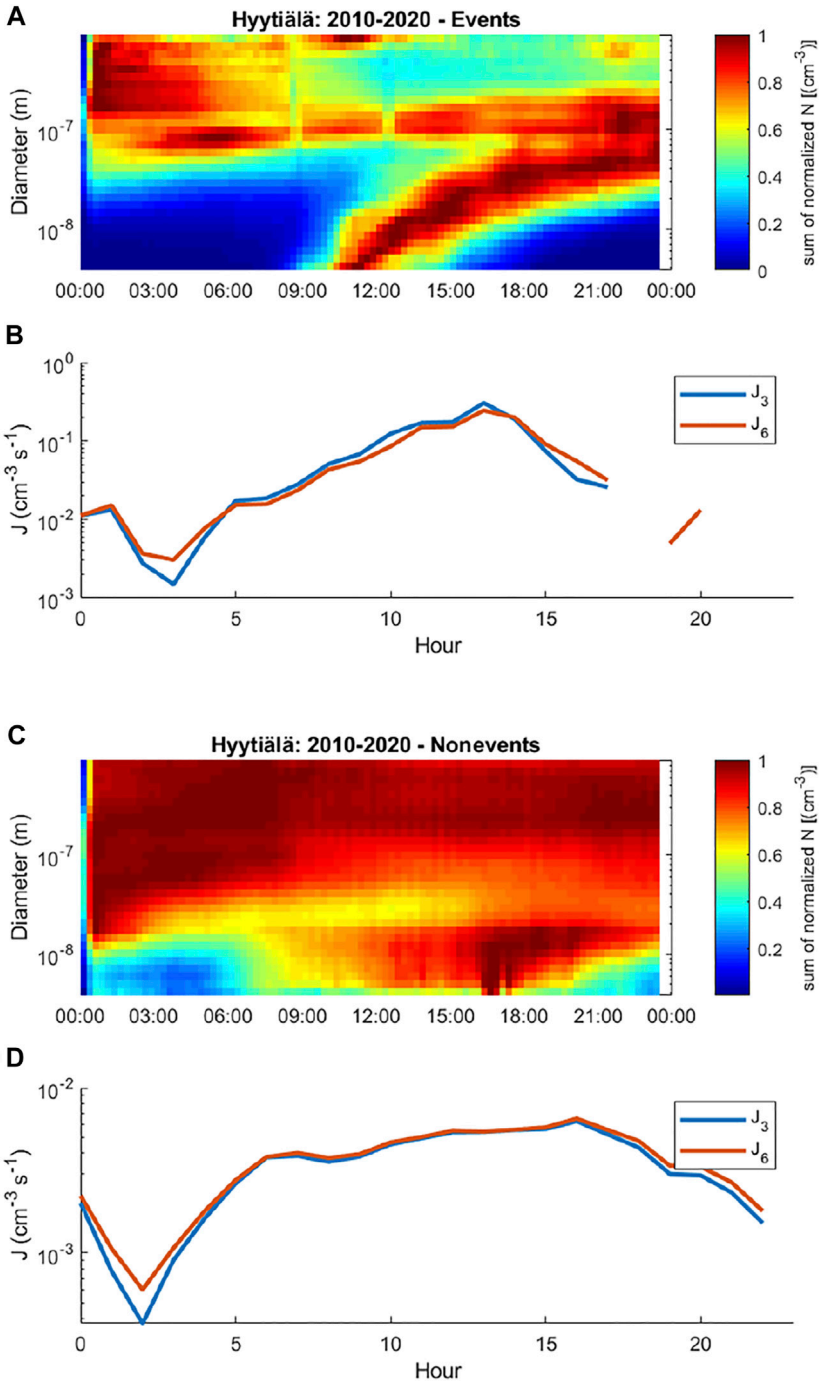

FIGURE 1 | Diurnal evolution of the particle number size distributions **(A,C)** and particle formation rates at formation rates at 3 and 6 nm **(B,D)** at the SMEAR II station in Hyytiälä, Finland. In particle number size distributions, each size bin was scaled individually between 0 and 1, and then averaged **(A)** over strong (Type Ia) NPF event days (21 days) and **(C)** over non-event days (1361 days). The signal of daytime NPF followed by new particle growth to larger sizes can be seen not only for NPF event days, but also for non-event days.

formation rates at 6 nm peaked at around noon on NPF event days. These features are similar to those observed in Hyytiälä. On the "average" non-event day, the formation rate of 6 nm particles peaked after the noon in Järveselja and Budapest near-city backgound, qualitatively similar to Hyytiälä, whereas in Budapest city center a more complicated pattern emerges. There, the particle formation rate is relatively high during most of the day, with somewhat higher values during the rush hours, suggesting that traffic emissions might contribute to quiet NPF at that site.

TABLE 1 | Ratios in the maximum (first column) and daily (second column) formation rates of 6 nm particles (J_6) between the traditional NPF event days (EV) and quiet NPF event (traditional non-event) days (non-EV), and growth rates (GR, nm h^{-1}) of 6–25 nm particles (third column) for both types of days, in the four atmospheric environments. The second data set of growth rates calculated with the maximum concentration method are given for Hyytiälä.

Sites	Ratio in Maximum J_6 Between EV and Non-EV	Ratio in Daily J_6 Between EV and Non-EV	GR (nm h^{-1}) for EV/For Non-EV
Hyytiälä	45	14.3	4.5/3.9 (4.3/2.9)
Järvselja	21	6.0	4.4/3.8
Budabest near-city background	13	3.6	7.4/6.1
Budapest city center	5	2.0	10.4/5.1

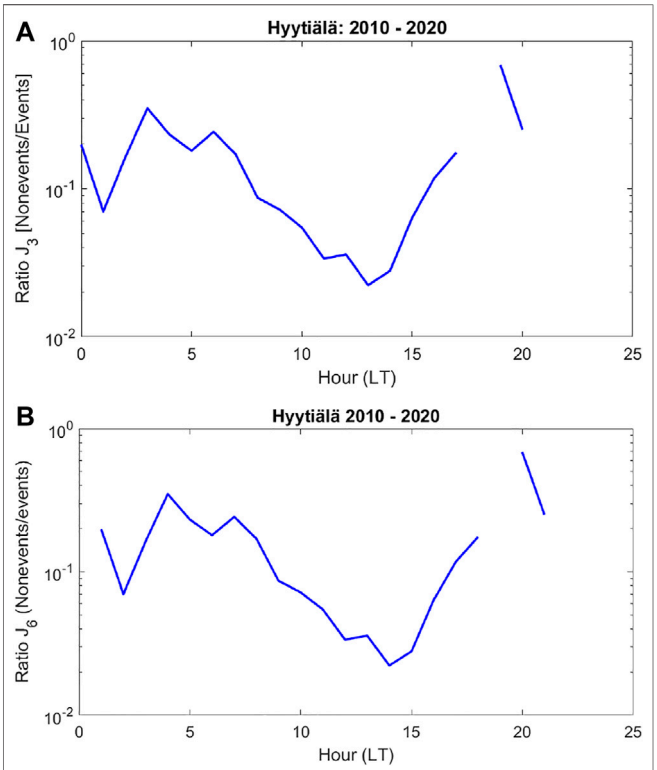

FIGURE 2 | The ratio in the formation rate of 3 nm **(A)** and 6 nm **(B)** particles between the quiet NPF (traditional non-event) days and traditional NPF event days at the SMEAR II station in Hyytiälä, Finland.

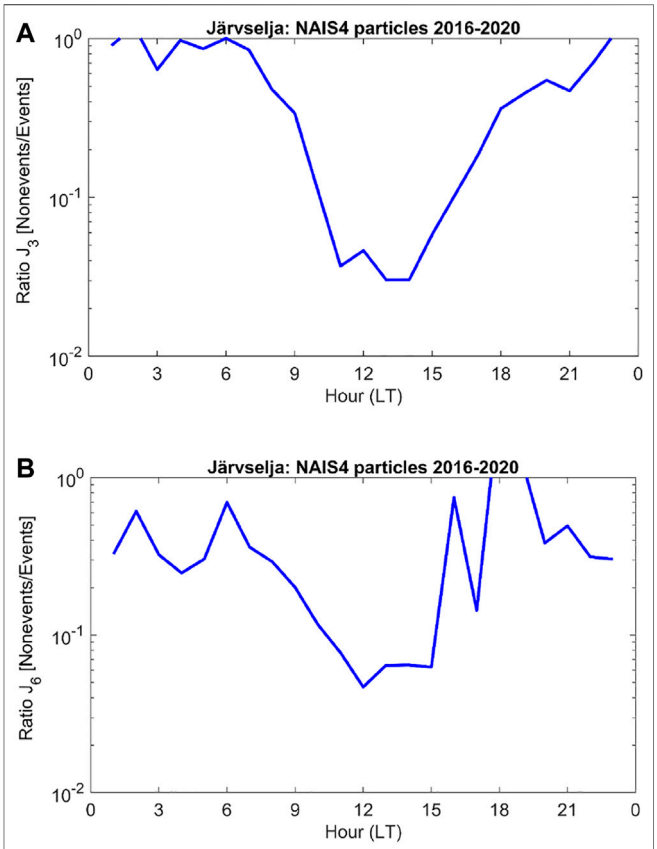

FIGURE 3 | The ratio in the formation rate of 3 nm **(A)** and 6 nm **(B)** particles between the quiet NPF (traditional non-event) days and traditional NPF event days at the SMEAR Estonia station in Järvselja, Estonia.

We then investigated the diurnal evolution of the average ratio in the particle formation rate between the non-event days and NPF event days at all the sites. In Hyytiälä, this ratio was mostly above 0.1 during nighttime for both J_3 and J_6, and in the range of about 0.02–0.2 during daytime (**Figure 2**). In Järvselja, the corresponding ratios were somewhat higher than those in Hyytiälä, being mostly above 0.3 during the nighttime and between about 0.03 and 0.3 during daytime (**Figure 3**). In Budapest, this ratio for J_6 was even higher than those in either Hyytiälä or Järvselja, fluctuating around unity from late afternoon until early morning, and being larger than about 0.05 (near-city background) or 0.2 (city center) during most of the daytime (**Figure 4**).

Overall, our observations show surprisingly small variability in average growth rates of nucleation mode particles between the NPF even and non-event days, as well as between the different sites, ranging from 3.9 (or 2.9 based on the maximum concentration method) nm h^{-1} (Hyytiälä non-event days) to 10.4 nm h^{-1} (Budapest city center, NPF event days). This is in line with our recent observations of generally limited variation in particle growth rates across different locations and conditions (Kulmala et al., 2022a; Stolzenburg et al., 2022). The differences in particle formation rates at 6 nm between the NPF event and non-event days were the largest in Hyytiälä, where biogenic sources

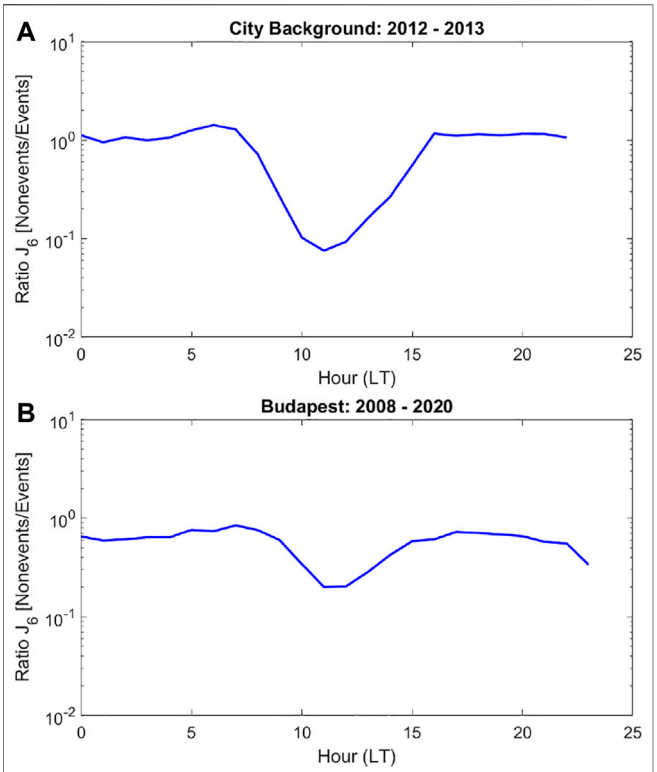

FIGURE 4 | The ratio in the formation rate of 6 nm particles between the quiet NPF (traditional non-event) days and traditional NPF event days at the near-city background site **(A)** and city center **(B)** of Budapest, Hungary.

are known to give an important contribution to NPF and subsequent growth of newly formed particles (e.g. Lehtipalo et al., 2018; Petäjä et al., 2022). The corresponding differences were the lowest in the Budapest city center, the site with the largest influence of anthropogenic pollution of the four sites considered here (Salma et al., 2017).

Importance of Quiet NPF as a Source for Particle Numbers

In order to estimate the relative importance of quiet and traditional NPF events as sources of new particles at our measurement sites, we calculated the daily production rate of 6 nm particles by integrating J_6 over the full diurnal cycle for both traditional NPF event days and quite NPF event days, and then taking into account the relative occurrence frequency of NPF event days and non-event days at each site (**Table 2**).

We estimated that the production rate of 6 nm particles per day varies from about 300 cm^{-3} (Hyytiälä, non-event days) to 70,000 cm^{-3} (Budapest city center, NPF event days; **Table 2**). Using the values from **Table 2** and assuming that 25% of days are NPF event days, we can see that in the conditions occurring in Hyytiälä on NPF event days produces about 4 times more particles than the other days in absolute terms. On the other hand, in Budapest, the quiet NPF event days seem to produce even more particles than the traditional NPF event days. The

TABLE 2 | Daily production rates (cm^{-3} d^{-1}) of 6–25 nm particles during traditional NPF event days and quiet NPF event (tradional non-event) days in the four atmospheric environments.

Sites	NPF Events	Non-events
Hyytiälä	4086	286
Järvselja	11109	1915
Budapest near-city background	18460	5080
Budapest city center	69800	35200

contribution of non-event days to all relevant days in the city center was 74%, whereas the occurrence frequency for NPF event days was 21%, and the remaining 5% were undefined days. The corresponding frequencies for the near-city background were 67, 28 and 5%. Since the daily particle production rate in Budapest city is around twice in event than in non-event days and there are 3.5 times more non-event days, the quiet nucleation produces almost twice as many particles during a year than the identified NPF event days. The number concentration of 6 nm particles produced during a day (**Table 2**) exceeds the median concentration of 6–25 nm at every site for both average NPF event and non-event day (**Supplementary Figure S10**). This provides further support for the atmospheric importance of traditional and quiet NPF in maintaining the sub-25 nm particle population, noting the typical lifetimes of these particles of the order of a few hours (Kwon et al., 2020).

Summarizing the calculations made above, we can state that the quiet NPF associated with traditional non-event days has a significant contribution to the total source strength of new 6 nm particles at our measurement sites, even approaching the values produced by the traditional NPF events under polluted conditions. The subsequent fate of these particles, and thereby their climatic and potential health effects, depends essentially on whether they can survive from coagulation scavenging into the pre-existing particle population during their growth to larger sizes. Although this survival probability is expected to be much higher than that of molecular clusters or sub-6 nm particles, it may be influential under polluted conditions or at low particle growth rates (Kerminen et al., 2001; Pierce and Adams, 2007; Kulmala et al., 2017; Kulmala et al., 2022b).

SUMMARY AND CONCLUSIONS

We have investigated a previously overlooked phenomenon: the formation of new aerosol particles during days when regional NPF (Mäkelä et al., 1997; Kerminen et al., 2018) seem not to occur, traditionally called non-event days. Already Tammet et al. (2013) and Tammet et al. (2014) investigated this phenomenon and suggested that it is called quiet NPF.

So far, NPF events are typically classified visually, based on the appearance of the nucleation mode. Therefore, if we cannot see the mode by eye in a figure representing the daily evolution of the particle number size distribution, the investigated day is classified as a non-event day. This feature is largely due to the used color scale in figures, and practically this color scale cannot be adjusted

to capture concentrations smaller than 10 particles cm^{-3} in the nucleation mode and simultaneously include the accumulation and cluster modes. When we normalize the particle number concentration in each size bin, we are can visually see the event (particle formation and subsequent growth), because the maximum concentration per size bin will appear even at particle number concentration well below 1 particles cm^{-3} in the nucleation mode. However, we need to integrate over several days in order to get rid of the noise, which is on top of the very low signal at the small sizes during non-event days.

We started our analysis using long-term continuous observations from the SMEAR II station in Hyytiälä, Finland, and tested the same method in Järvselja (Estonia) and Budapest (Hungary) where relatively long time series are also available. We found that a banana-type particle growth similar to NPF event days can be seen at all the sites after averaging over a number of traditional non-event days. Furthermore, we found that the average formation rates at 6 nm during daytime on quiet NPF events varied between about 2% and >50% of the corresponding formation rates on traditional NPF event days (**Figures 2–4**; **Table 1**), the percentage being higher in more polluted environments. We estimated that the daily production rate of 6 nm particles is 2–15 times higher on traditional NPF event days compared with quiet NPF event days, depending on the sites (**Tables 2**). Since this quiet NPF occurs more frequently than traditional NPF, there are potentially several regions or cities on the Earth—such as Budapest—where the quiet NPF seems to be a more important source of new particles than the traditional NPF. In very clean atmospheric environments such as Hyytiälä and Järvselja, in which biogenic sources for the precursors of NPF are crucial, the traditional regional NPF events are probably still dominating atmospheric new particle production. With an increasing anthropogenic influence, the quiet NPF (i.e. traditional non-event) days seem to give a significant contribution to atmospheric aerosol production.

If we look at GTP from a clustering point of view, we can say that the clustering occurs—in practice—every day and night (Kulmala et al., 2013; Kontkanen et al., 2017). Here we observed that the growth rate of newly formed particles is relatively similar between the traditional NPF event and quiet NPF event days at each site, while earlier observations have shown surprisingly small variability in GR during NPF events observed around the world (e.g. Kulmala et al., 2022b). The fact that the GR is relatively invariable indicates that in atmospheric NPF, the most crucial step is the activation of existing clusters for subsequent growth, determining the particle formation rate at a few nm. Therefore, the key question for further studies is: which mechanisms cause the activation of existing clusters?

Besides cluster activation, there are other priorites for future work related to quiet NPF. First, one should explore what instrumental and analytical developments or refinements are needed to investigate this phenomenon quantitative in different environments. Second, the work conducted here should be expanded to other environments, especially polluted megacities and other kinds of rural or remote areas. Third, one should investigate whether the clustering and cluster activation mechanisms of quiet NPF are similar or different to those during traditional NPF events. An issue related to this topic is, for example, the role of ion-induced NPF. Finally, further studies are needed on the climate and air quality importance of quiet NPF in comparison with traditional NPF, especially when it comes to the further growth of particles from a few nm to CCN and haze particle sizes both regionally and on the global scale.

DATA AVAILABILITY STATEMENT

The raw data supporting the conclusion of this article will be made available by the authors, without undue reservation.

AUTHOR CONTRIBUTIONS

MK and HJ has the idea. MK and V-MK developed the idea. HJ made the first algorithm. All contributed to obtaining the data and analysing it. MK and V-MK drafted the MS. All contributed the writing.

FUNDING AND ACKNOWLEDGEMENTS

We acknowledge the following projects: ACCC Flagship funded by the Academy of Finland grant number 337549, Academy professorship funded by the Academy of Finland (Grant Nos. 302958), Academy of Finland projects no. 1325656, 311932, 316114, 332547, and 325647; "Quantifying carbon sink, CarbonSink+ and their interaction with air quality" INAR project funded by Jane and Aatos Erkko Foundation, European Research Council (ERC) project ATM-GTP Contract No. 742206, Samsung PM2.5 SRP, the European Union's Horizon 2020 research and innovation programme Marie Skłodowska-Curie grant agreement no. 895875 ("NPF-PANDA") and the Marie Skłodowska-Curie ITN "CLOUD-MOTION" (764991), the Hungarian Research, Development and Innovation Office (K132254), New National Excellence Program of the Ministry for Innovation and Technology, Hungary (ÚNKP-21-3), European Regional Development Fund (project MOBTT42) under the Mobilitas Pluss programme, Estonian Research Council (project PRG714), Estonian Environmental Observatory (KKOBS, project 2014-2020.4.01.20-0281). Technical and scientific staff in Hyytiälä, Järvselja and Budapest are acknowledged.

SUPPLEMENTARY MATERIAL

The Supplementary Material for this article can be found online at: https://www.frontiersin.org/articles/10.3389/fenvs.2022.912385/full#supplementary-material

Supplementary Figure S1 | Time evolution of the particle number size distribution averaged over NPF event days during a 10-year period (1997–2007) at the SMEAR II station in Hyytiälä, Finland. The data includes 973 NPF event days. The color indicates the particle number concentration ($dN/d\log D_p$).

Supplementary Figure S2 | Time evolution of the particle number size distribution averaged over non-event days during a 10-year period (1997–2007) at the SMEAR II station in Hyytiälä, Finland. The data includes 1184 non-event days. The color indicates the particle number concentration ($dN/d\log D_p$).

Supplementary Figure S3 | Averaged NPF event days, so that each size bin has been scaled individually between 0 and 1. Data is from a 10-year period (1997–2007) at the SMEAR II station in Hyytiälä, Finland. This shows that maximum concentration of each size bin is shifting to later hours during the day, and this corresponds to growth of particles over the course of an average day. The color indicates the normalized number concentration in each size bin (like in **Figure 1**).

Supplementary Figure S4 | Averaged non-event, each size bin scaled individually between 0 and 1. Data is from a 10-year period (1997–2007) at the SMEAR II station in Hyytiälä, Finland. This shows that maximum concentration for particles smaller than 30 nm is shifting to later hours during the day, and this corresponds to growth for particles over the course of an average non-event day. The color indicates the normalized number concentration in each size bin (like in **Figure 1**).

Supplementary Figure S5 | Time for the maxima of the normalized particle number concentration (normalized signal) in individual size bins occur later during the day for larger-diameter size bins, providing direct indication of particle growth. Due to low particle formation rates, we cannot detect this effect for a single non-NPF day, but only when averaged over long time (hundreds of individual non-NPF days). Data is from a 10-year period (1997–2007) at the SMEAR II station in Hyytiälä, Finland.

Supplementary Figure S6 | Time of maximum concentrations in the size bins averaged over non-event days shown in **Supplementary Figure S5**. A linear fit to the data gives a growth rate of 2.9 nm h^{-1}.

Supplementary Figure S7 | Normalized NPF events (left panels) and traditional non-events (quiet NPF events, right panels) in Budapest city center during 2008–2020.

Supplementary Figure S8 | Normalized NPF events (left panels) and traditional non-events (quiet NPF events, right panels) in Budapest near-city background during 2012–2013.

Supplementary Figure S9 | Normalized air ion number concentration distribution plots and intermediate ion (diameter 2–8 nm) concentrations (red line = positive ions, blue line = negative ions) in Järvselja during 2016–2020. The plots were used to calculate the average GR of newly formed particles on NPF event days of type Ia (top panel, 38 days, $GR_{6\text{-}25}$ = 4.4 nm h^{-1}) and non-event (bottom panel, 749 days, $GR_{6\text{-}25}$ = 3.8 nm h^{-1}).

Supplementary Figure S10 | Atmospheric concentrations of 6–25 nm particles at each measurement site calculated for the same periods as in **Figures 2–4**. The red line represents the median of the data and the lower and upper edges of the box represent 25th and 75th percentiles of the data, respectively. The length of the whiskers represents 1.5 × the interquartile range which includes 99.3% of the data. Data outside the whiskers are considered outliers and are marked with red crosses.

REFERENCES

Aalto, P., Hämeri, K., Becker, E., Weber, R., Salm, J., Mäkelä, J. M., et al. (2001). Physical Characterization of Aerosol Particles during Nucleation Events. *Tellus B Chem. Phys. Meteorol.* 53, 344–358. doi:10.3402/tellusb.v53i4.17127

Apte, J. S., Marshall, J. D., Cohen, A. J., and Brauer, M. (2015). Addressing Global Mortality from Ambient PM2.5. *Environ. Sci. Technol.* 49, 8057–8066. doi:10.1021/acs.est.5b01236

Arneth, A., Unger, N., Kulmala, M., and Andreae, M. O. (2009). Clean the Air, Heat the Planet? *Science* 326, 672–673. doi:10.1126/science.1181568

Boucher, O., Randall, D., Artaxo, P., Bretherton, C., Feingold, G., Forster, P., et al. (2013). "Clouds and Aerosols," in *Climate Change 2013: The Physical Science Basis. Contribution of Working Group I to the Fifth Assessment Report of the Intergovernmental Panel on Climate Change*. Editors T. Stocker, D. Qin, G. Plattner, M. Tignor, S. Allen, J. Boschung, et al. (Cambridge, United Kingdom and New York, NY, USA: Cambridge University Press).

Bousiotis, D., Brean, J., Pope, F. D., Dall'Osto, M., Querol, X., Alastuey, A., et al. (2021). The Effect of Meteorological Conditions and Atmospheric Composition in the Occurrence and Development of New Particle Formation (NPF) Events in Europe. *Atmos. Chem. Phys.* 21, 3345–3370. doi:10.5194/acp-21-3345-2021

Buenrostro Mazon, S., Riipinen, I., Schultz, D. M., Valtanen, M., Dal Maso, M., Sogacheva, L., et al. (2009). Classifying Previously Undefined Days from Eleven Years of Aerosol-Particle-Size Distribution Data from the SMEAR II Station, Hyytiälä, Finland. *Atmos. Chem. Phys.* 9, 667–676. doi:10.5194/acp-9-667-2009

Cai, R., Jiang, J., Mirme, S., and Kangasluoma, J. (2019). Parameters Governing the Performance of Electrical Mobility Spectrometers for Measuring Sub-3 Nm Particles. *J. Aerosol Sci.* 127, 102–115. doi:10.1016/j.jaerosci.2018.11.002

Chu, B., Kerminen, V.-M., Bianchi, F., Yan, C., Petäjä, T., and Kulmala, M. (2019). Atmospheric New Particle Formation in China. *Atmos. Chem. Phys.* 19, 115–138. doi:10.5194/acp-19-115-2019

Dada, L., Chellapermal, R., Buenrostro Mazon, S., Paasonen, P., Lampilahti, J., Manninen, H. E., et al. (2018). Refined Classification and Characterization of Atmospheric New-Particle Formation Events Using Air Ions. *Atmos. Chem. Phys.* 18, 17883–17893. doi:10.5194/acp-18-17883-2018

Dada, L., Lehtipalo, K., Kontkanen, J., Nieminen, T., Baalbaki, R., Ahonen, L., et al. (2020). Formation and Growth of Sub-3-nm Aerosol Particles in Experimental Chambers. *Nat. Protoc.* 15, 1013–1040. doi:10.1038/s41596-019-0274-z

Dada, L., Paasonen, P., Nieminen, T., Buenrostro Mazon, S., Kontkanen, J., Peräkylä, O., et al. (2017). Long-Term Analysis of Clear-Sky New Particle Formation Events and Nonevents in Hyytiälä. *Atmos. Chem. Phys.* 17, 6227–6241. doi:10.5194/acp-17-6227-2017

Dai, L., Wang, H., Zhou, L., An, J., Tang, L., Lu, C., et al. (2017). Regional and Local New Particle Formation Events Observed in the Yangtze River Delta Region, China. *J. Geophys. Res. Atmos.* 122, 2389–2402. doi:10.1002/2016JD026030

Dal Maso, M., Kulmala, M., Riipinen, I., and Wagner, R. (2005). Formation and Growth of Fresh Atmospheric Aerosols: Eight Years of Aerosol Size Distribution Data from SMEAR II, Hyytiälä, Finland. *Boreal Environ. Res.* 10, 323–336.

Deng, C., Cai, R., Yan, C., Zheng, J., and Jiang, J. (2021). Formation and Growth of Sub-3 Nm Particles in Megacities: Impact of Background Aerosols. *Faraday Discuss.* 226, 348–363. doi:10.1039/D0FD00083C

Fiore, A. M., Naik, V., Spracklen, D. V., Steiner, A., Unger, N., Prather, M., et al. (2012). Global Air Quality and Climate. *Chem. Soc. Rev.* 41, 6663–6683. doi:10.1039/C2CS35095E

Gordon, H., Kirkby, J., Baltensperger, U., Bianchi, F., Breitenlechner, M., Curtius, J., et al. (2017). Causes and Importance of New Particle Formation in the Present-Day and Preindustrial Atmospheres. *J. Geophys. Res. Atmos.* 122, 8739–8760. doi:10.1002/2017JD026844

Hari, P., and Kulmala, M. (2005). Station for Measuring Ecosystem-Atmosphere Relations (SMEAR II). *Boreal Environ. Res.* 10, 315–322.

Hirsikko, A., Laakso, L., Hõrrak, U., Aalto, P., Kerminen, V.-M., and Kulmala, M. (2005). Annual and Size Dependent Variation of Growth Rates and Ion Concentrations in Boreal Forest. *Boreal Env. Res.* 10 (5), 357–369.

Hussein, T., Junninen, H., Tunved, P., Kristensson, A., Dal Maso, M., Riipinen, I., et al. (2009). Time Span and Spatial Scale of Regional New Particle Formation Events Over Finland and Southern Sweden. *Atmos. Chem. Phys.* 9, 4699–4716. doi:10.5194/acp-9-4699-2009

Iida, K., Stolzenburg, M., McMurry, P., Dunn, M. J., Smith, J. N., Eisele, F., et al. (2006). Contribution of Ion-Induced Nucleation to New Particle Formation: Methodology and its Application to Atmospheric Observations in Boulder, Colorado. *J. Geophys. Res.* 111, D23201. doi:10.1029/2006JD007167

IPCC (2021). Summary for Policymakers. In *Climate Change 2021: The Physical Science Basis. Contribution of Working Group I to the Sixth Assessment Report of the Intergovernmental Panel on Climate Change*. Editors V. Masson-Delmotte, P. Zhai, A. Pirani, S. L. Connors, C. Péan, S. Berger, et al. (Cambridge: Cambridge University Press), pp. 3-32. doi:10.1017/9781009157896.001

Junninen, H., Ahonen, L., Bianchi, F., Quelever, L., Schallhart, S., Dada, L., et al. (2022). Terpene Emissions from Boreal Wetlands Can Initiate Stronger Atmospheric New Particle Formation Than Boreal Forests. *Nat. Commun. Earth Environ.* 3, 93. doi:10.1038/s43247-022-00406-9

Kalkavouras, P., BougiatiotI, A., Hussein, T., Kalivitis, N., Stavroulas, I., Michalopoulos, P., et al. (2021). Regional New Particle Formation over the Eastern Mediterranean and Middle East. *Atmosphere* 12, 13. doi:10.3390/atmos12010013

Kangasluoma, J., Cai, R., Jiang, J., Deng, C., Stolzenburg, D., Ahonen, L. R., et al. (2020). Overview of Measurements and Current Instrumentation for 1-10 Nm Aerosol Particle Number Size Distributions. *J. Aerosol Sci.* 148, 105584. doi:10.1016/j.jaerosci.2020.105584

Kerminen, V.-M., Anttila, T., Petäjä, T., Laakso, L., Gagne, S., Lehtinen, K. E. J., et al. (2007). "Using Charging State in Estimating the Relative Importance of Neutral and Ion-Induced Nucleation," in *Nucleation and Atmospheric Aerosols*. Editors C.D. O'Dowd and P.E. Wagner (Dordrecht: Springer), 350–353. doi:10.1007/978-1-4020-6475-3_71

Kerminen, V.-M., Chen, X., Vakkari, V., Petäjä, T., Kulmala, M., and Bianchi, F. (2018). Atmospheric New Particle Formation and Growth: Review of Field Observations. *Environ. Res. Lett.* 13, 103003. doi:10.1088/1748-9326/aadf3c

Kerminen, V.-M., Pirjola, L., and Kulmala, M. (2001). How Significantly Does Coagulational Scavenging Limit Atmospheric Particle Production? *J. Geophys. Res.* 106, 24119–24125. doi:10.1029/2001JD000322

Kontkanen, J., Lehtipalo, K., Ahonen, L., Kangasluoma, J., Manninen, H. E., Hakala, J., et al. (2017). Measurements of Sub-3 Nm Particles Using a Particle Size Magnifier in Different Environments: from Clean Mountain Top to Polluted Megacities. *Atmos. Chem. Phys.* 17, 2163–2187. doi:10.5194/acp-17-2163-2017

Kulmala, M., Dada, L., Daellenbach, K. R. K., Yan, C., Stolzenburg, D., Kontkanen, J., et al. (2021). Is Reducing New Particle Formation a Plausible Solution to Mitigate Particulate Air Pollution in Beijing and Other Chinese Megacities? *Faraday Discuss.* 226, 334–347. doi:10.1039/D0FD00078G

Kulmala, M., Cai, R., Stolzenburg, D., Zhou, Y., Dada, L., Guo, Y., et al. (2022b). The Contribution of New Particle Formation and Subsequent Growth to Haze Formation. *Environ. Sci. Atmos.* 2, 352–361. doi:10.1039/D1EA00096A

Kulmala, M., Kerminen, V.-M., Anttila, T., Laaksonen, A., and O'Dowd, C. D. (2004b). Organic Aerosol Formation *via* Sulphate Cluster Activation. *J. Geophys. Res.* 109, D04205. doi:10.1029/2003JD003961

Kulmala, M., and Kerminen, V.-M. (2008). On the Formation and Growth of Atmospheric Nanoparticles. *Atmos. Res.* 90, 132–150. doi:10.1016/j.atmosres.2008.01.005

Kulmala, M., Kerminen, V.-M., Petäjä, T., Ding, A. J. A., and Wang, L. (2017). Atmospheric Gas-To-Particle Conversion: Why NPF Events Are Observed in Megacities? *Faraday Discuss.* 200, 271–288. doi:10.1039/C6FD00257A

Kulmala, M., Kontkanen, J., Junninen, H., Lehtipalo, K., Manninen, H. E., Nieminen, T., et al. (2013). Direct Observations of Atmospheric Aerosol Nucleation. *Science* 339, 943–946. doi:10.1126/science.1227385

Kulmala, M., Petäjä, T., Nieminen, T., Sipilä, M., Manninen, H. E., Lehtipalo, K., et al. (2012). Measurement of the Nucleation of Atmospheric Aerosol Particles. *Nat. Protoc.* 7, 1651–1667. doi:10.1038/nprot.2012.091

Kulmala, M., Stolzenburg, D., Dada, L., Cai, R., Kontkanen, J., Yan, C., et al. (2022a). Towards a Concentration Closure of Sub-6 Nm Aerosol Particles and Sub-3 Nm Atmospheric Clusters. *J. Aerosol Sci.* 159, 105878. doi:10.1016/j.jaerosci.2021.105878

Kulmala, M., Vehkamäki, H., Petäjä, T., Dal Maso, M., Lauri, A., Kerminen, V.-M., et al. (2004a). Formation and Growth Rates of Ultrafine Atmospheric Particles: A Review of Observations. *J. Aerosol Sci.* 35, 143–176. doi:10.1016/j.jaerosci.2003.10.003

Kwon, H.-S., Ryu, M. H., and Carlsten, C. (2020). Ultrafine Particles: Unique Physicochemical Properties Relevant to Health and Disease. *Exp. Mol. Med.* 52, 318–328. doi:10.1038/s12276-020-0405-1

Lehtipalo, K., Kontkanen, J., Kangasluoma, J., Franchin, A., Wimmer, D., Schobesberger, S., et al. (2014). Methods for Determining Particle Size Distribution and Growth Rates between 1 and 3 Nm Using the Particle Size Magnifier. *Boreal Environ. Res.* 19, 215–236.

Lehtipalo, K., Yan, C., Dada, L., Bianchi, F., Xiao, M., Wagner, R., et al. (2018). Multicomponent New Particle Formation from Sulfuric Acid, Ammonia, and Biogenic Vapors. *Sci. Adv.* 4, eaau5363. doi:10.1126/sciadv.aau5363

Mäkelä, J. M., Aalto, P., Jokinen, V., Pohja, T., Nissinen, A., Palmroth, S., et al. (1997). Observations of Ultrafine Aerosol Particle Formation and Growth in Boreal Forest. *Geophys. Res. Lett.* 24, 1219–1222. doi:10.1029/97gl00920

Manninen, H. E., Petäjä, T., Asmi, E., Riipinen, I., Nieminen, T., Mikkilä, J., et al. (2009). Long-Term Field Measurements of Charged and Neutral Clusters Using Neutral Cluster and Air Ion Spectrometer (NAIS). *Boreal Environ. Res.* 14, 591–605.

McMurry, P. H., and Friedlander, S. K. (1979). New Particle Formation in the Presence of an Aerosol. *Atmos. Environ.* 13, 1635–1651. doi:10.1016/0004-6981(79)90322-6

Mirme, A., Tamm, E., Mordas, G., Vana, M., Uin, J., Mirme, S., et al. (2007). A Wide-Range Multi-Channel Air Ion Spectrometer. *Boreal Environ. Res.* 12, 247–264.

Mirme, S., and Mirme, A. (2013). The Mathematical Principles and Design of the NAIS - a Spectrometer for the Measurement of Cluster Ion and Nanometer Aerosol Size Distributions. *Atmos. Meas. Tech.* 6, 1061–1071. doi:10.5194/amt-6-1061-2013

Németh, Z., Rosati, B., Zíková, N., Salma, I., Bozó, L., Dameto de España, C., et al. (2018). Comparison of Atmospheric New Particle Formation Events in Three Central European Cities. *Atmos. Environ.* 178, 191–197. doi:10.1016/j.atmosenv.2018.01.035

Németh, Z., and Salma, I. (2014). Spatial Extension of Nucleating Air Masses in the Carpathian Basin. *Atmos. Chem. Phys.* 14, 8841–8848. doi:10.5194/acp-14-8841-2014

Nieminen, T., Asmi, A., Dal Maso, M., Aalto, P., Keronen, P., Petaja, T., et al. (2014). Trends in Atmospheric New-Particle Formation: 16 Years of Observations in a Boreal-Forest Environment. *Boreal Environ. Res.* 19, 191–214.

Nieminen, T., Kerminen, V.-M., Petäjä, T., Aalto, P. P., Arshinov, M., Asmi, E., et al. (2018). Global Analysis of Continental Boundary Layer New Particle Formation Based on Long-Term Measurements. *Atmos. Chem. Phys.* 18, 14737–14756. doi:10.5194/acp-18-14737-2018

Noe, S. M., Kimmel, V., Hüve, K., Copolovici, L., Portillo-Estrada, M., Püttsepp, Ü., et al. (2011). Ecosystem-Scale Biosphere-Atmosphere Interactions of a Hemiboreal Mixed Forest Stand at Järvselja, Estonia. *For. Ecol. Manag.* 262, 71–81. doi:10.1016/j.foreco.2010.09.013

Noe, S. M., Niinemets, Ü., Krasnova, A., Krasnov, D., Motallebi, A., Kängsepp, V., et al. (2015). SMEAR Estonia: Perspectives of a Large-Scale Forest Ecosystem - Atmosphere Research Infrastructure. *For. Stud.* 63, 56–84. doi:10.1515/fsmu-2015-0009

Petäjä, T., Tabakova, K., Manninen, A., Ezhova, E., O'Connor, E., Moisseev, D., et al. (2022). Influence of Biogenic Emissions from Boreal Forests on Aerosol-Cloud Interactions. *Nat. Geosci.* 15, 42–47. doi:10.1038/s41561-021-00876-0

Philip, S., Martin, R. V., van Donkelaar, A., Lo, J. W.-H., Wang, Y., Chen, D., et al. (2014). Global Chemical Composition of Ambient Fine Particulate Matter for Exposure Assessment. *Environ. Sci. Technol.* 48, 13060–13068. doi:10.1021/es502965b

Pierce, J. R., and Adams, P. J. (2007). Efficiency of Cloud Condensation Nuclei Formation from Ultrafine Particles. *Atmos. Chem. Phys.* 7, 1367–1379. doi:10.5194/acp-7-1367-2007

Pöschl, U. (2005). Atmospheric Aerosols: Composition, Transformation, Climate and Health Effects. *Angew. Chem. Int. Ed.* 44, 7520–7540. doi:10.1002/anie.200501122

Rose, C., Collaud Coen, M., Andrews, E., Lin, Y., Bossert, I., Lund Myhre, C., et al. (2021). Seasonality of the Particle Number Concentration and Size Distribution: A Global Analysis Retrieved from the Network of Global Atmosphere Watch (GAW) Near-Surface Observatories. *Atmos. Chem. Phys.* 21, 17185–17223. doi:10.5194/acp-21-17185-2021

Salma, I., and Németh, Z. (2019). Dynamic and Timing Properties of New Aerosol Particle Formation and Consecutive Growth Events. *Atmos. Chem. Phys.* 19, 5835–5852. doi:10.5194/acp-19-5835-2019

Salma, I., Németh, Z., Kerminen, V.-M., Aalto, P., Nieminen, T., Weidinger, T., et al. (2016b). Regional Effect on Urban Atmospheric Nucleation. *Atmos. Chem. Phys.* 16, 8715–8728. doi:10.5194/acp-16-8715-2016

Salma, I., Németh, Z., Weidinger, T., Kovács, B., and Kristóf, G. (2016a). Measurement, Growth Types and Shrinkage of Newly Formed Aerosol Particles at an Urban Research Platform. *Atmos. Chem. Phys.* 16, 7837–7851. doi:10.5194/acp-16-7837-2016

Salma, I., Thén, W., Aalto, P., Kerminen, V.-M., Kern, A., Barcza, Z., et al. (2021). Influence of Vegetation on Occurrence and Time Distributions of Regional New Aerosol Particle Formation and Growth. *Atmos. Chem. Phys.* 21, 2861–2880. doi:10.5194/acp-21-2861-2021

Salma, I., Varga, V., and Németh, Z. (2017). Quantification of an Atmospheric Nucleation and Growth Process as a Single Source of Aerosol Particles in a City. *Atmos. Chem. Phys.* 17, 15007–15017. doi:10.5194/acp-17-15007-2017

Samset, B. H. (2018). How Cleaner Air Changes the Climate. *Science* 360, 148–150. doi:10.1126/science.aat1723

Spracklen, D. V., Carslaw, K. S., Kulmala, M., Kerminen, V.-M., Mann, G. W., and Sihto, S.-L. (2006). The Contribution of Boundary Layer Nucleation Events to Total Particle Concentrations on Regional and Global Scales. *Atmos. Chem. Phys.* 6, 5631–5648. doi:10.5194/acp-6-5631-2006

Stolzenburg, D., Ozon, M., Kulmala, M., Lehtinen, K. E. J., Lehtipalo, K., and Kangasluoma, J. (2022). Combining Instrument Inversions for Sub-10 Nm Aerosol Number Size-Distribution Measurements. *J. Aerosol Sci.* 159, 105862. doi:10.1016/j.jaerosci.2021.105862

Stolzenburg, D., Steiner, G., and Winkler, P. M. (2017). A DMA-Train for Precision Measurement of Sub-10 Nm Aerosol Dynamics. *Atmos. Meas. Tech.* 10, 1639–1651. doi:10.5194/amt-10-1639-2017

Tammet, H., Komsaare, K., and Hõrrak, U. (2013). Estimating Neutral Nanoparticle Steady-State Size Distribution and Growth According to Measurements of Intermediate Air Ions. *Atmos. Chem. Phys.* 13, 9597–9603. doi:10.5194/acp-13-9597-2013

Tammet, H., Komsaare, K., and Hõrrak, U. (2014). Intermediate Ions in the Atmosphere. *Atmos. Res.* 135-136, 263–273. doi:10.1016/j.atmosres.2012.09.009

Tammet, H., Mirme, A., and Tamm, E. (2002). Electrical Aerosol Spectrometer of Tartu University. *Atmos. Res.* 62, 315–324. doi:10.1016/S0169-8095(02)00017-0

Tröstl, J., Chuang, W. K., Gordon, H., Heinritzi, M., Yan, C., Molteni, U., et al. (2016). The Role of Low-Volatility Organic Compounds in Initial Particle Growth in the Atmosphere. *Nature* 533, 527–531. doi:10.1038/nature18271

Tuovinen, S., Kontkanen, J., Jiang, J., and Kulmala, M. (2020). Investigating the Effectiveness of Condensation Sink Based on Heterogeneous Nucleation Theory. *J. Aerosol Sci.* 149, 105613. doi:10.1016/j.jaerosci.2020.105613

Wang, Z., Wu, Z., Yue, D., Shang, D., Guo, S., Sun, J., et al. (2017). New Particle Formation in China: Current Knowledge and Further Directions. *Sci. Total Environ.* 577, 258–266. doi:10.1016/j.scitotenv.2016.10.177

Weagle, C. L., Snider, G., Li, C., van Donkelaar, A., Philip, S., Bissonnette, P., et al. (2018). Global Sources of Fine Particulate Matter: Interpretation of PM2.5 Chemical Composition Observed by SPARTAN Using a Global Chemical Transport Model. *Environ. Sci. Technol.* 52, 11670–11681. doi:10.1021/acs.est.8b01658

Wiedensohler, A., Birmili, W., Nowak, A., Sonntag, A., Weinhold, K., Merkel, M., et al. (2012). Mobility Particle Size Spectrometers: Harmonization of Technical Standards and Data Structure to Facilitate High Quality Long-Term Observations of Atmospheric Particle Number Size Distributions. *Atmos. Meas. Tech.* 5, 657–685. doi:10.5194/amt-5-657-2012

Yu, F., and Luo, G. (2009). Simulation of Particle Size Distribution with a Global Aerosol Model: Contribution of Nucleation to Aerosol and CCN Number Concentrations. *Atmos. Chem. Phys.* 9, 7691–7710. doi:10.5194/acp-9-7691-2009

Conflict of Interest: The authors declare that the research was conducted in the absence of any commercial or financial relationships that could be construed as a potential conflict of interest.

Publisher's Note: All claims expressed in this article are solely those of the authors and do not necessarily represent those of their affiliated organizations, or those of the publisher, the editors and the reviewers. Any product that may be evaluated in this article, or claim that may be made by its manufacturer, is not guaranteed or endorsed by the publisher.

Supplementary figures

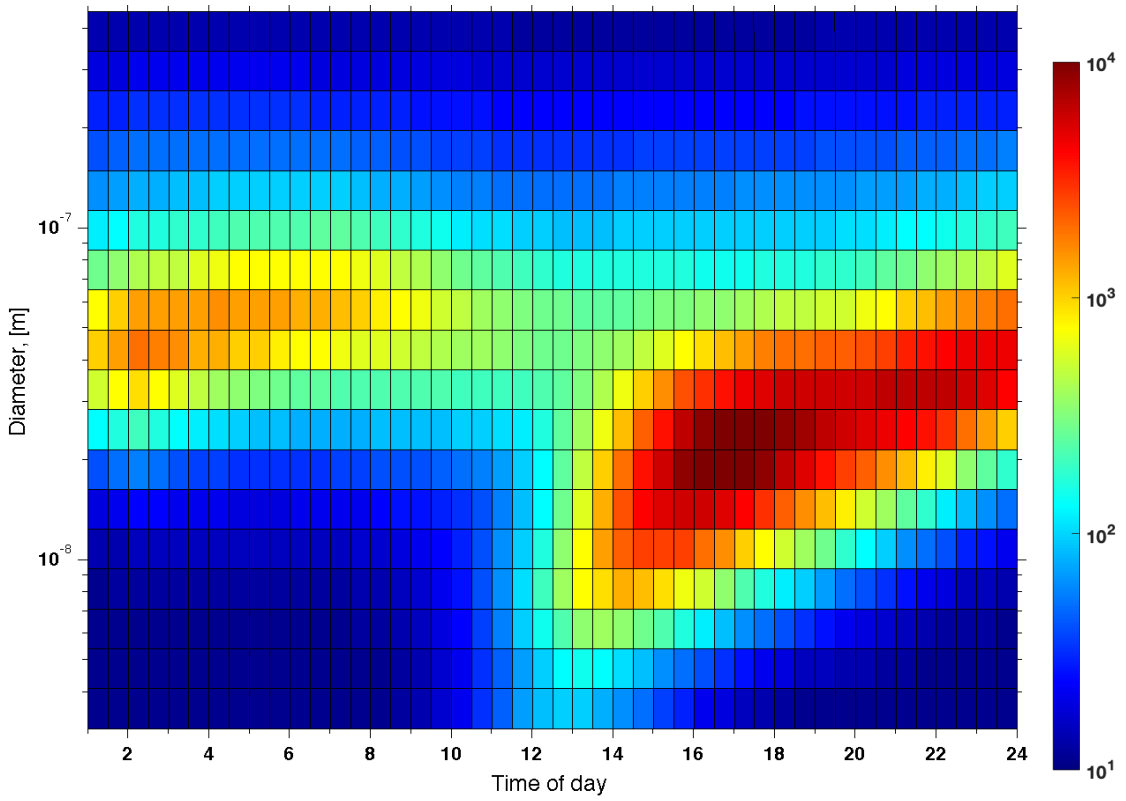

Figure S1. Time evolution of the particle number size distribution averaged over NPF event days during a 10-year period (1997–2007) at the SMEAR II station in Hyytiälä, Finland. The data includes 973 NPF event days. The color indicates the particle number concentration ($dN/d\log D_p$).

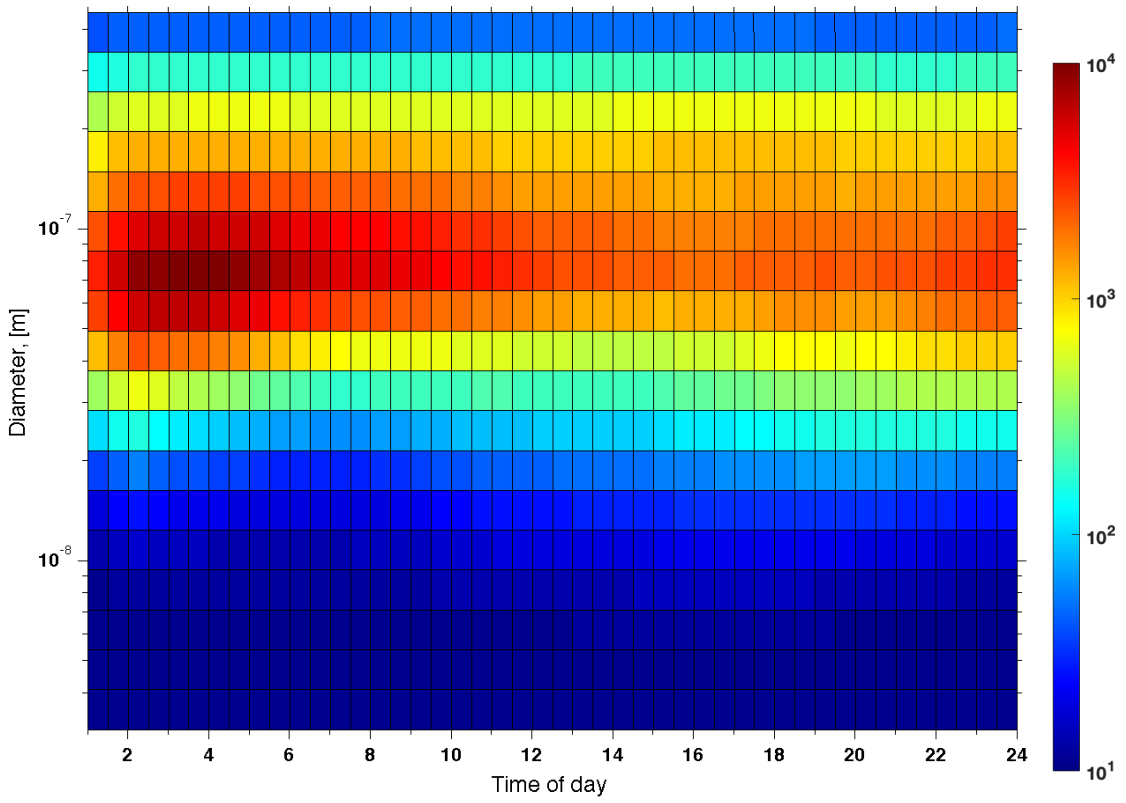

Figure S2. Time evolution of the particle number size distribution averaged over non-event days during a 10-year period (1997–2007) at the SMEAR II station in Hyytiälä, Finland. The data includes 1 184 non-event days. The color indicates the particle number concentration (dN/dlogD_p).

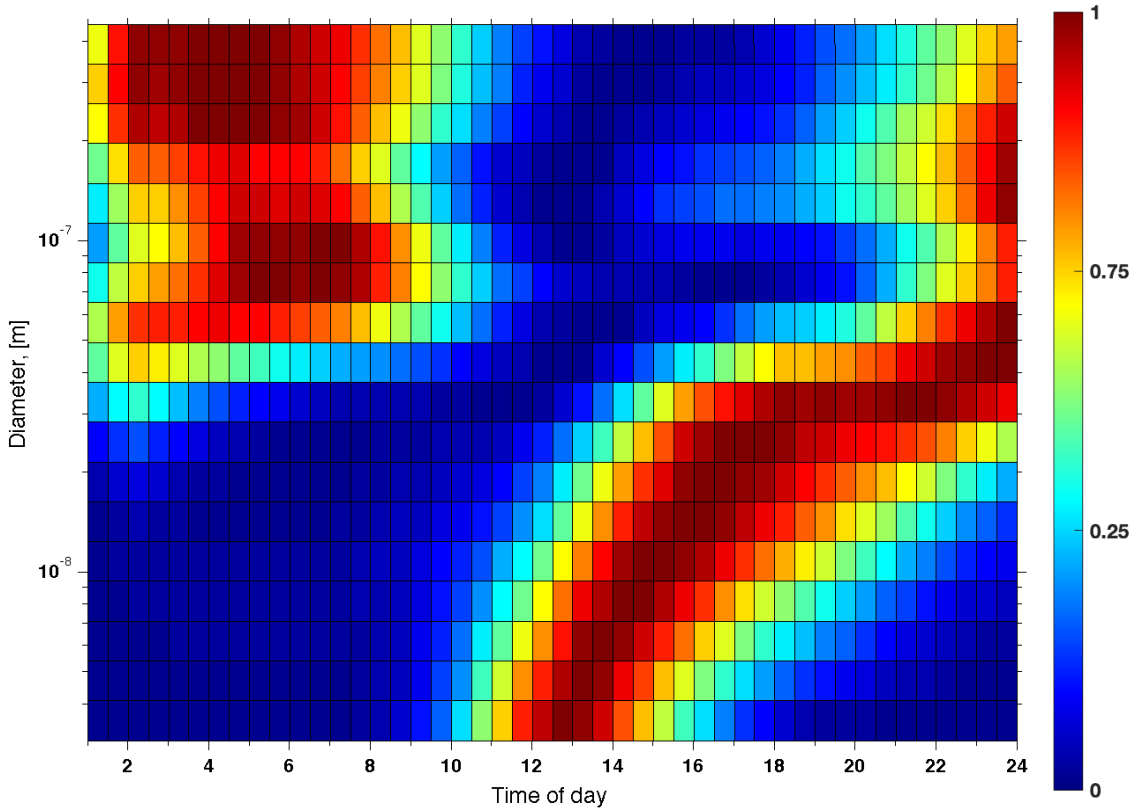

Figure S3. Averaged NPF event days, so that each size bin has been scaled individually between 0 and 1. Data is from a 10-year period (1997–2007) at the SMEAR II station in Hyytiälä, Finland. This shows that maximum concentration of each size bin is shifting to later hours during the day, and this corresponds to growth of particles over the course of an average day. The color indicates the normalized number concentration in each size bin (like in Figure 1).

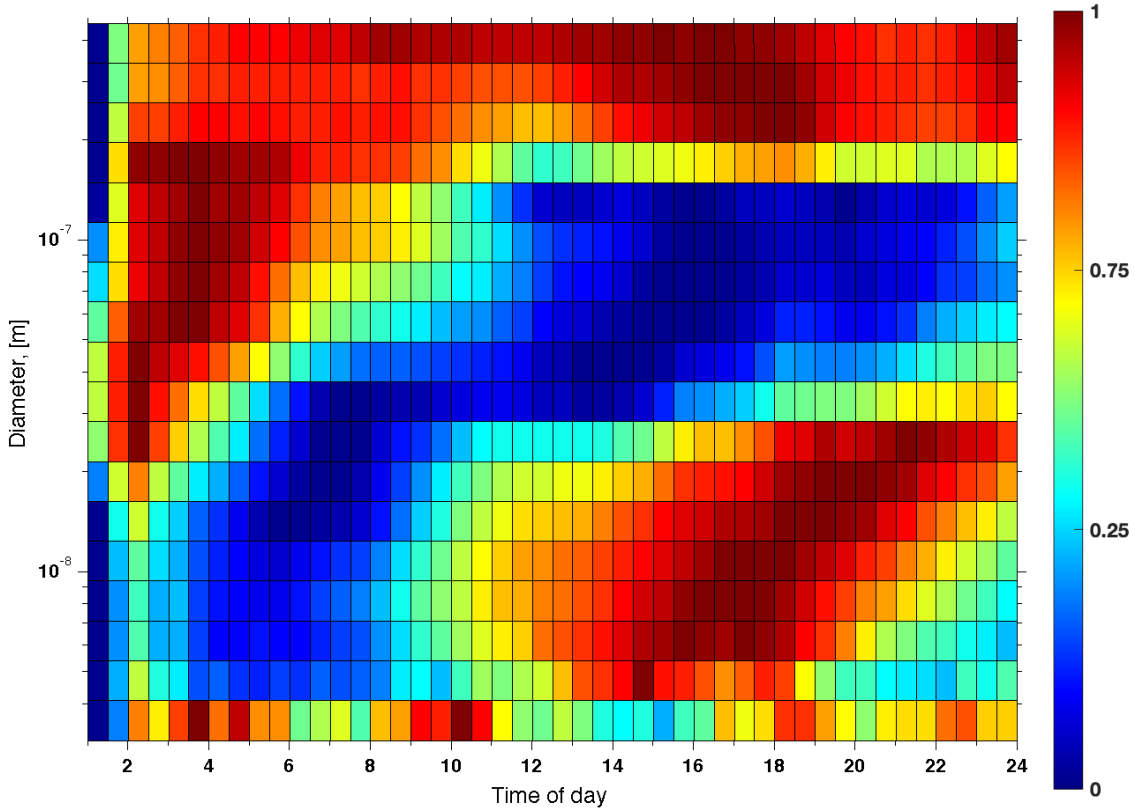

Figure S4. Averaged non-event, each size bin scaled individually between 0 and 1. Data is from a 10-year period (1997–2007) at the SMEAR II station in Hyytiälä, Finland. This shows that maximum concentration for particles smaller than 30 nm is shifting to later hours during the day, and this corresponds to growth for particles over the course of an average non-event day. The color indicates the normalized number concentration in each size bin (like in Figure 1).

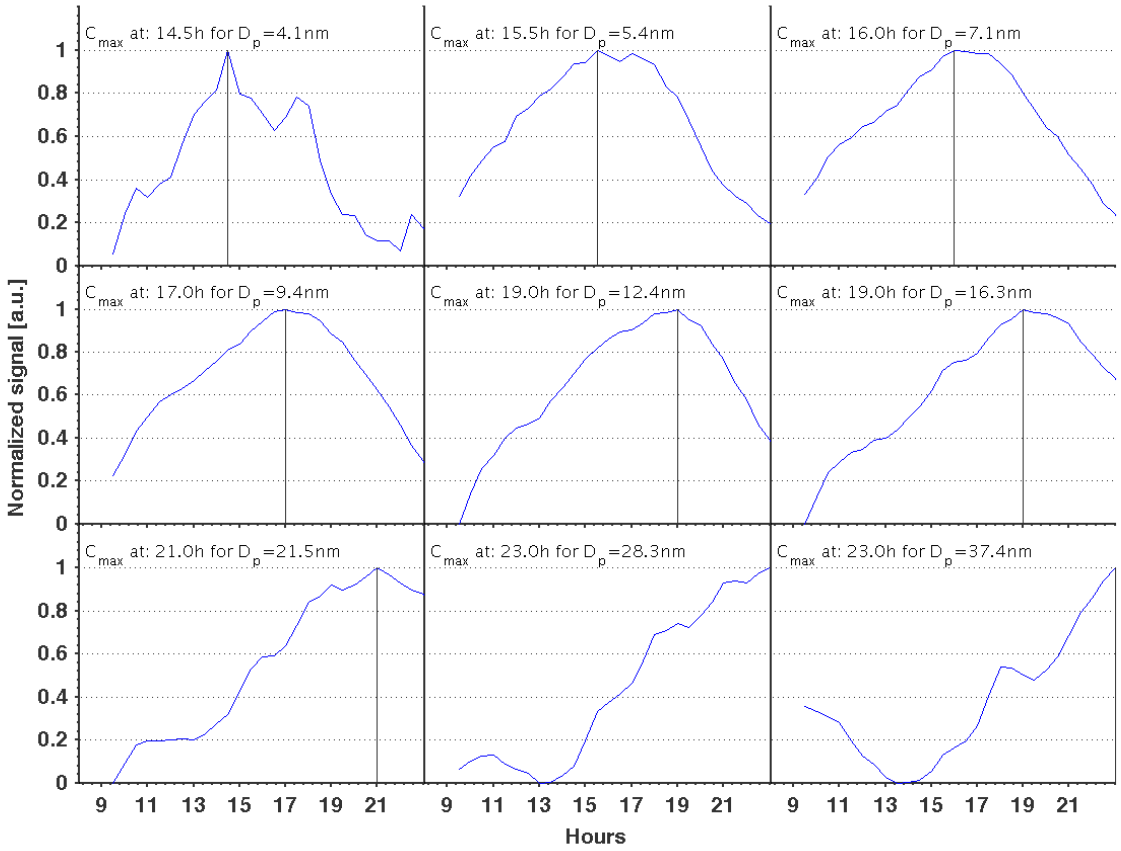

Figure S5. Time for the maxima of the normalized particle number concentration (normalized signal) in individual size bins occur later during the day for larger-diameter size bins, providing direct indication of particle growth. Due to low particle formation rates, we cannot detect this effect for a single non-NPF day, but only when averaged over long time (hundreds of individual non-NPF days). Data is from a 10-year period (1997–2007) at the SMEAR II station in Hyytiälä, Finland.

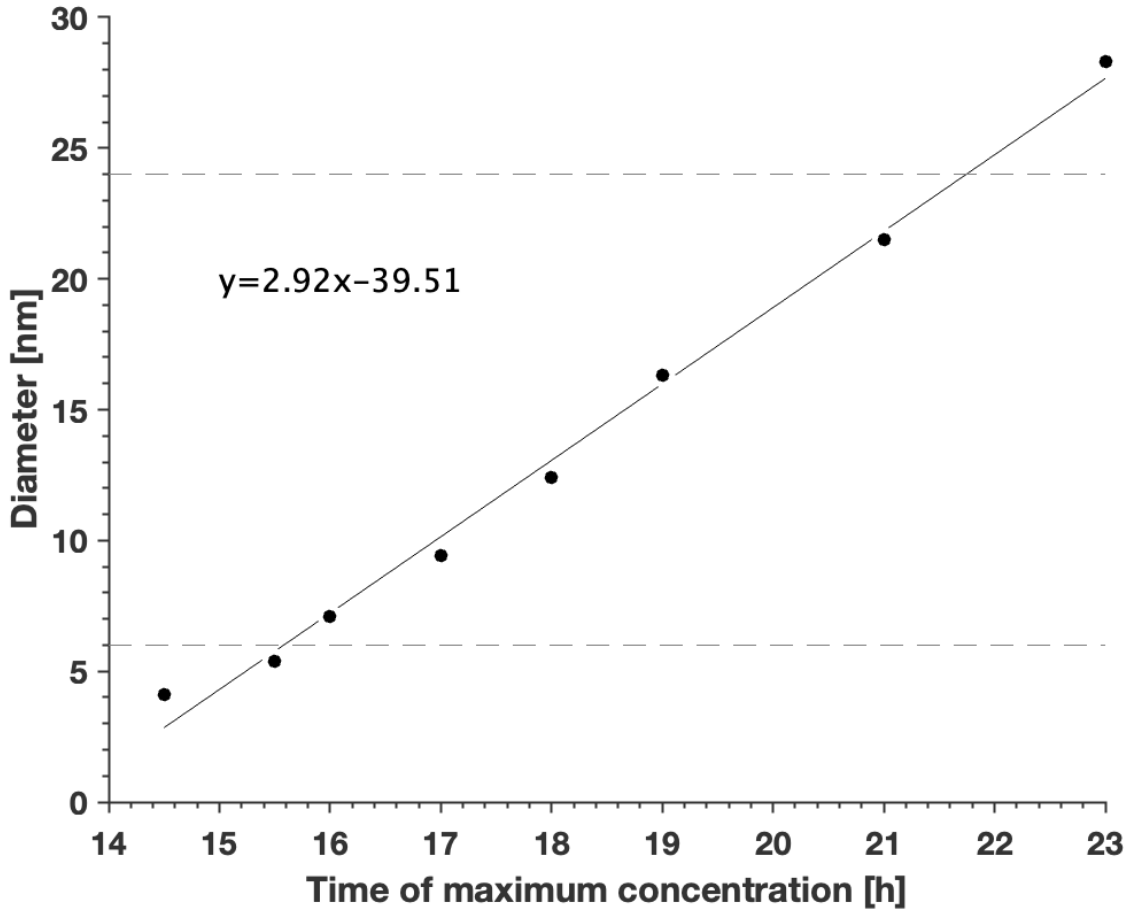

Figure S6. Time of maximum concentrations in the size bins averaged over non-event days shown in Supplementary Figure S5. A linear fit to the data gives a growth rate of 2.9 nm h^{-1}.

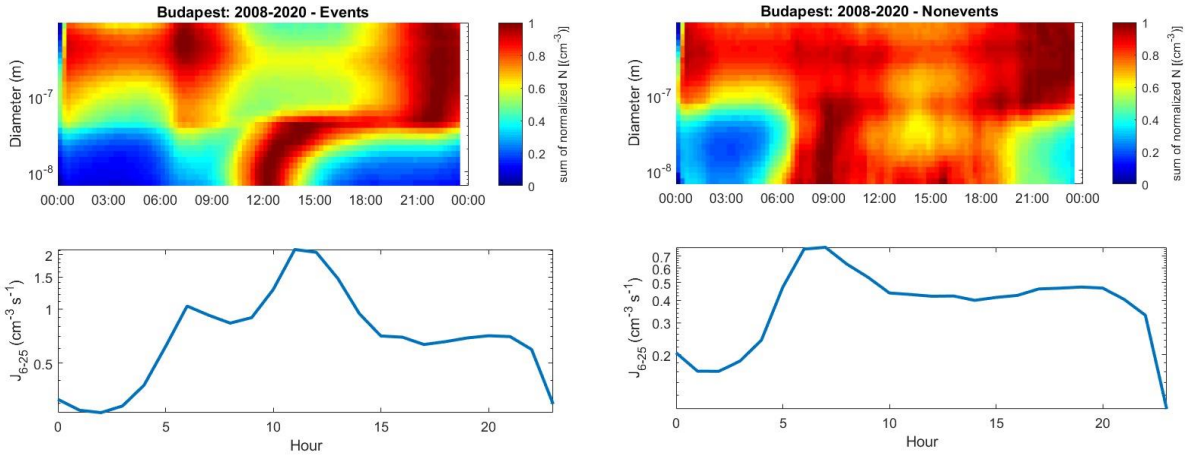

Figure S7. Normalized NPF events (left panels) and traditional non-events (quiet NPF events, right panels) in Budapest city center during 2008–2020.

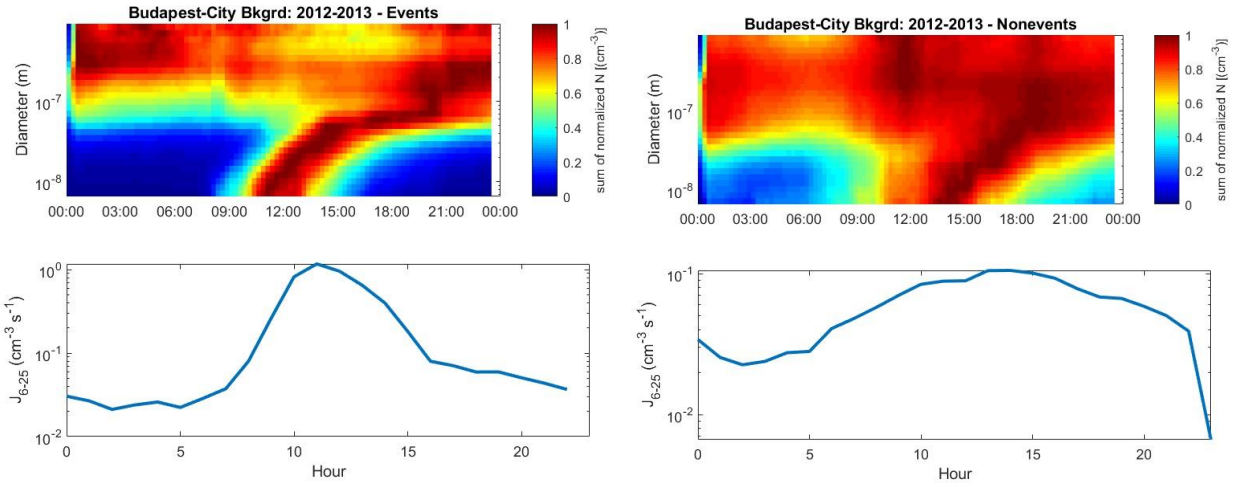

Figure S8. Normalized NPF events (left panels) and traditional non-events (quiet NPF events, right panels) in Budapest near-city background during 2012–2013.

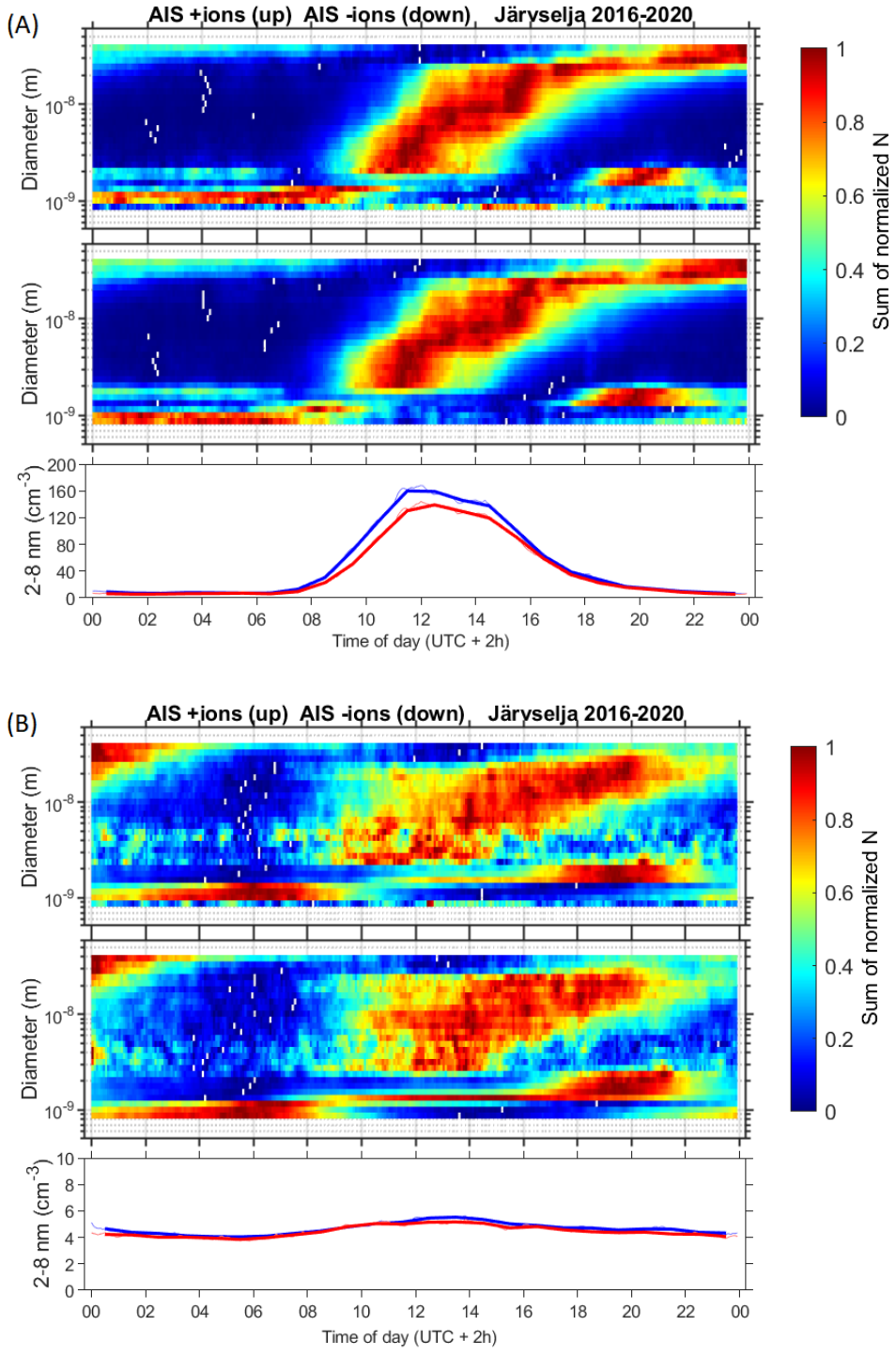

Figure S9. Normalized air ion number concentration distribution plots and intermediate ion (diameter 2–8 nm) concentrations (red line = positive ions, blue line = negative ions) in Järvselja during 2016–2020. The plots were used to calculate the average GR of newly formed particles on NPF event days of type Ia (top panel, 38 days, $GR_{6–25}$ = 4.4 nm h^{-1}) and non-event days (bottom panel, 749 days, $GR_{6–25}$ = 3.8 nm h^{-1}).

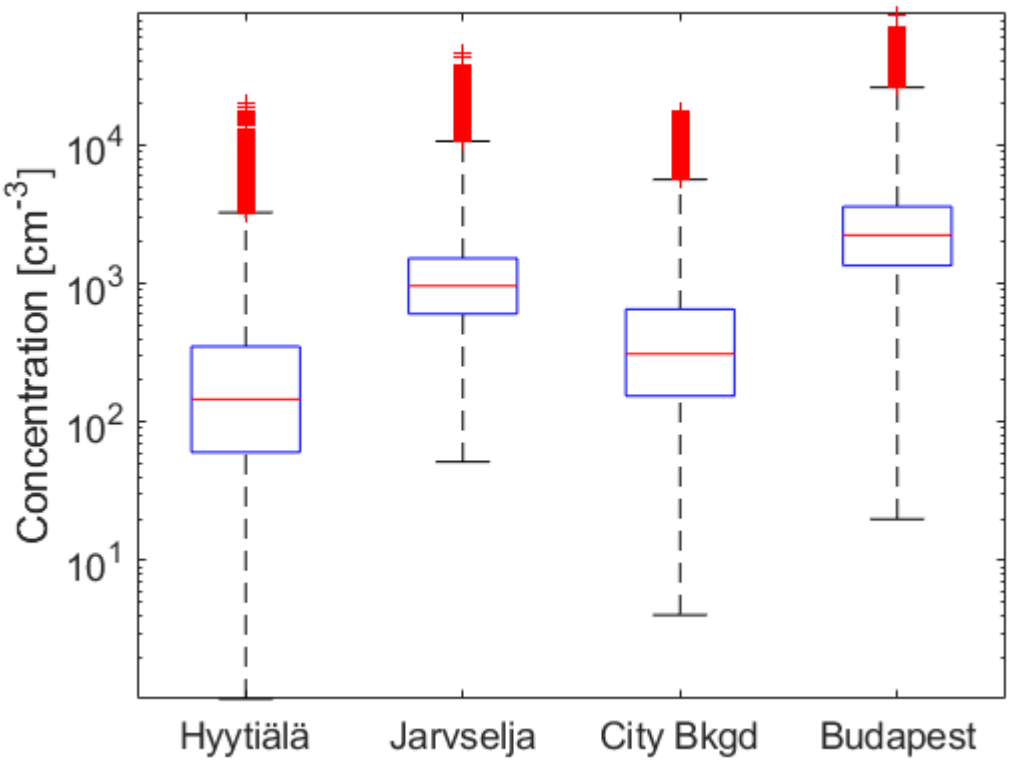

Figure S10. Atmospheric concentrations of 6–25 nm particles at each measurement site calculated for the same periods as in Figures 2–4. The red line represents the median of the data and the lower and upper edges of the box represent 25th and 75th percentiles of the data, respectively. The length of the whiskers represent 1.5 × the interquartile range which includes 99.3 % of the data. Data outside the whiskers are considered outliers and are marked with red crosses.